



## Distributed Bragg reflectors based on diluted boron-based BAlN alloys for deep ultraviolet optoelectronic applications

M. Abid, T. Moudakir, G. Orsal, S. Gautier, A. En Naciri, Zakaria Djebbour, J.H. Ryou, G. Patriarche, L. Largeau, H. J. Kim, et al.

### ► To cite this version:

M. Abid, T. Moudakir, G. Orsal, S. Gautier, A. En Naciri, et al.. Distributed Bragg reflectors based on diluted boron-based BAlN alloys for deep ultraviolet optoelectronic applications. Applied Physics Letters, 2012, 100 (5), pp.051101. 10.1063/1.3679703 . hal-00666779

**HAL Id: hal-00666779**

**<https://hal.science/hal-00666779>**

Submitted on 2 Dec 2021

**HAL** is a multi-disciplinary open access archive for the deposit and dissemination of scientific research documents, whether they are published or not. The documents may come from teaching and research institutions in France or abroad, or from public or private research centers.

L'archive ouverte pluridisciplinaire **HAL**, est destinée au dépôt et à la diffusion de documents scientifiques de niveau recherche, publiés ou non, émanant des établissements d'enseignement et de recherche français ou étrangers, des laboratoires publics ou privés.

# Distributed Bragg reflectors based on diluted boron-based BAlN alloys for deep ultraviolet optoelectronic applications

M. Abid,<sup>1</sup> T. Moudakir,<sup>1</sup> G. Orsal,<sup>2</sup> S. Gautier,<sup>2</sup> A. En Naciri,<sup>3</sup> Z. Djebbour,<sup>4,5</sup> J.-H. Ryou,<sup>6</sup> G. Patriarche,<sup>7</sup> L. Largeau,<sup>7</sup> H. J. Kim,<sup>6</sup> Z. Lochner,<sup>6</sup> K. Pantzas,<sup>1</sup> D. Alamarguy,<sup>4</sup> F. Jomard,<sup>8</sup> R. D. Dupuis,<sup>6</sup> J.-P. Salvestrini,<sup>2</sup> P. L. Voss,<sup>1</sup> and A. Ougazzaden<sup>1,a)</sup>

<sup>1</sup>Georgia Institute of Technology/GT-Lorraine-UMI 2958 Georgia Tech-CNRS, 2-3 rue Marconi, 57070 Metz, France

<sup>2</sup>Laboratoire Matériaux Optiques, Photonique et Système (LMOPS), EA 4423, Université Paul Verlaine et Supélec/UMI 2958 Georgia Tech-CNRS, 2 rue E. Belin, 57070 Metz, France

<sup>3</sup>Laboratoire de Physique des Milieux Denses (LPMO), Université Paul Verlaine-Metz, 1 boulevard Arago, 57070 Metz, France

<sup>4</sup>Laboratoire de Génie Electrique de Paris (LGE), UMR 8507 CNRS, Supélec, Université Paris-Sud 11, Université Pierre et Marie Curie, 11 rue Joliot-Curie, 91192 Gif-sur-Yvette Cedex, France

<sup>5</sup>Department of Physics and Engineering Science, University of Versailles (UVSQ), 45 Av. Des Etats Unis, 78035 Versailles, France

<sup>6</sup>Center for Compound Semiconductors and School of Electrical and Computer Engineering, Georgia Institute of Technology, Atlanta, Georgia 30332, USA

<sup>7</sup>LPN CNRS, UPR, Route de Nozay, F-91460 Marcoussy, France

<sup>8</sup>Laboratoire de Physique des solides et de Cristallogénèse (LPSC), UMR 8635 CNRS, University of Versailles-Saint-Quentin1, place Artstide Briand, 92195 Meudon Cedex, France

(Received 1 July 2011; accepted 6 January 2012; published online 30 January 2012)

Highly reflective deep UV distributed Bragg reflectors (DBRs) based on the BAlN material system have been grown by metalorganic vapour phase epitaxy on AlN template substrates. These structures make use of the transparency of BAlN in the deep UV and the high refractive index contrast between BAlN and AlN, which has been demonstrated to exceed 0.27 at 280 nm. 18-pair BAlN/AlN DBRs showed experimental peak reflectivity of 82% at 311 nm and a stop-bandwidth of 20 nm. At 282 nm, a 24-pair BAlN/AlN DBR structure is demonstrated with experimental peak reflectivity of 60% and stop-bandwidth of 16 nm. © 2012 American Institute of Physics. [doi:10.1063/1.3679703]

Highly reflective distributed Bragg reflectors (DBRs) are essential components for the development of deep-UV photonics devices such as vertical-cavity surface-emitting lasers (VCSELs). UV lasers have application in high density optical storage, medical diagnosis, and chemical and biological sensing, and advances in devices technology enable these applications. Substantial progress has been made in the last years in the UV and deep-UV light emitting devices based on AlGaIn materials.<sup>1,2</sup> Additionally, AlGaIn systems were intensively investigated to develop DBR structures in the UV region. However, these designs must carefully balance competing trade-offs. Factors to take into account include (a) the limited refractive index contrast that decreases with decreasing Ga content in the AlGaIn layers, (b) the transparency of the AlGaIn layers diminishes with increasing Ga content, and (c) the in-plane lattice mismatch of 2.4% between GaN and AlN which limits achievable film thickness. These competing requirements mean that high-reflectivity AlGaIn/AlGaIn DBRs need multilayer stacks with many periods and/or high Al concentrations favourable for plastic relaxation and to cracks generation, degrading the device quality and limiting its performance. Additionally, these systems suffer from reduced bandwidth limited by the weak refractive index contrast. To overcome these listed issues, nearly lattice matched AlInN/AlGaIn structures have recently been proposed as an al-

ternative approach.<sup>3,4</sup> In fact, the AlInN materials were recently proposed as a promising candidate for DBR structures and UV light emitting devices.<sup>5,6</sup> However, these AlInN-based DBRs are not efficient for VCSEL applications due to numerous ramping processes during the growth and the sensitivity of indium incorporation to the growth temperature. As a consequence, there have been relatively few reports studying DBR reflectivity below 320 nm.<sup>7,8</sup> However, the reported structures exhibited stop-bandwidths less than 13 nm. As a consequence of the difficulty to develop highly reflective DBRs with broad bandwidth, no VCSEL operating in the deep UV has been demonstrated.

Motivated by an experiment which provided some evidence of strong refractive index modification by 2% boron inclusion in AlN layers,<sup>9</sup> and also by the fact that the BAlN system should exhibit less optical absorption than the AlGaIn system, we study more thoroughly the refractive index of BAlN materials and we argue for the potential use of this material system for the development of versatile DBRs in a wide range of UV wavelengths with broad bandwidth. We have also fabricated promising BAlN based-DBRs, which demonstrate peak reflectivities of 82% at 311 nm and 60% at 282 nm. Although these results are currently comparable to the state-of-the-art deep UV results on nitrides-based DBR structures,<sup>7,8</sup> there is still potential for improvement to achieve higher reflectivities.

Growth was performed at 1000 °C on 0.9 μm thick AlN on sapphire templates in a low pressure MOVPE system

<sup>a)</sup> Author to whom correspondence should be addressed. Electronic mail: abdallah.ougazzaden@georgiatech-metz.fr.

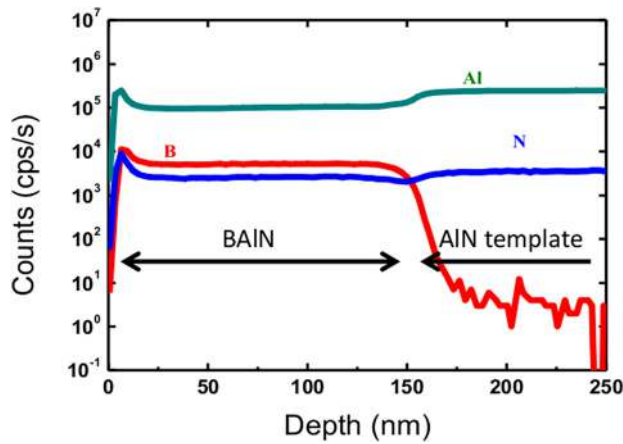


FIG. 1. (Color online) SIMS elemental concentration depth profiles for the B, Al, and N signal for the  $B_{0.34}Al_{0.66}N$  layers on AlN template.

using nitrogen as a carrier gas.<sup>10</sup> Trimethylaluminium (TMAI), triethylboron (TEB) III-group precursors, and ammonia were used as aluminium, boron, and nitrogen sources, respectively. Typical thickness of the grown BAIN layers for optical and material characterization was around 140 nm, deduced from *in-situ* laser reflectometry measurements.

An accurate knowledge of optical properties is essential for DBR and laser design. This knowledge is derived from a systematically grown series of samples in which the TEB/III molar ratio in the vapour phase was varied between 0% and 71% in order to vary the solid phase boron incorporation. First, XPS measurement estimated the boron content in the solid phase to vary between 0% and 47%. Then, the boron content calculation was confirmed by EDX analysis. In fact, although boron, a low-mass-element, cannot be detected by EDX, the composition was estimated by measuring the aluminium and considering the stoichiometry between the III and V elements. The XPS compositions were therefore confirmed. In order to evaluate the depth concentration profiles for Al, B, and N, secondary ion mass spectroscopy (SIMS) analysis was carried out on the BAIN films.

Figure 1 shows uniform boron distribution in one BAIN layer, along the growth direction, while in the BAIN layer, the aluminium concentration varies anti-phase with boron. This is an indication that the mixing of Al and B atoms occurs on the sub-lattice of III sites to form an alloy.

Ellipsometry measurements were used to investigate optical properties of BAIN, especially dispersion of refractive index ( $n$ ) at different wavelengths as well as the bandgap energy which is paramount for BAIN transparency. Data was acquired in the wavelength range of 200–800 nm at 70° incidence by using a phase modulator ellipsometer (from HORIBA Scientific). The ellipsometer evaluates  $I_c$  and  $I_s$ , which are linked to ellipsometric angles ( $\Psi, \Delta$ ) by  $I_c = \sin(2\Psi)\cos(\Delta)$  and  $I_s = \sin(2\Psi)\sin(\Delta)$ . The measured quantities were then fit to data generated from a model representing the sample. We applied the Jellison-Modin approach based on the Tauc-Lorentz (TL) model, which has been proven to be an efficient model for interpreting the ellipsometry spectra.<sup>11–13</sup> In addition, the Levenberg-Marquardt algorithm is used to minimizing the Mean Square Error  $\chi^2$ , the error function between experimental and calculated data; the latter were extracted from the physical model described as a five-layer ( $Al_2O_3$ /AlN/BAIN/roughness/air) system. The 150 nm-thick BAIN films exhibited 4–5 nm RMS roughness for the different boron content, measured by atomic force microscopy (AFM). This surface roughness was incorporated into the model.

Figure 2 shows experimental and calculated  $I_c$  and  $I_s$  versus the wavelength for several BAIN samples. The good agreement between experimental (dotted lines) and calculated (solid lines) spectra and the reasonable  $\chi^2$  value indicate that the assumed model and the obtained data are reliable.

Figure 3 presents the resulting refractive index data for the BAIN films as derived from the ellipsometry fits. The different optical bandgaps calculated from the ellipsometric fit are summarized in Table I. The calculation of the boron content corresponding to the TEB/III ratios is also reported in this table. The demonstrated high optical bandgap values

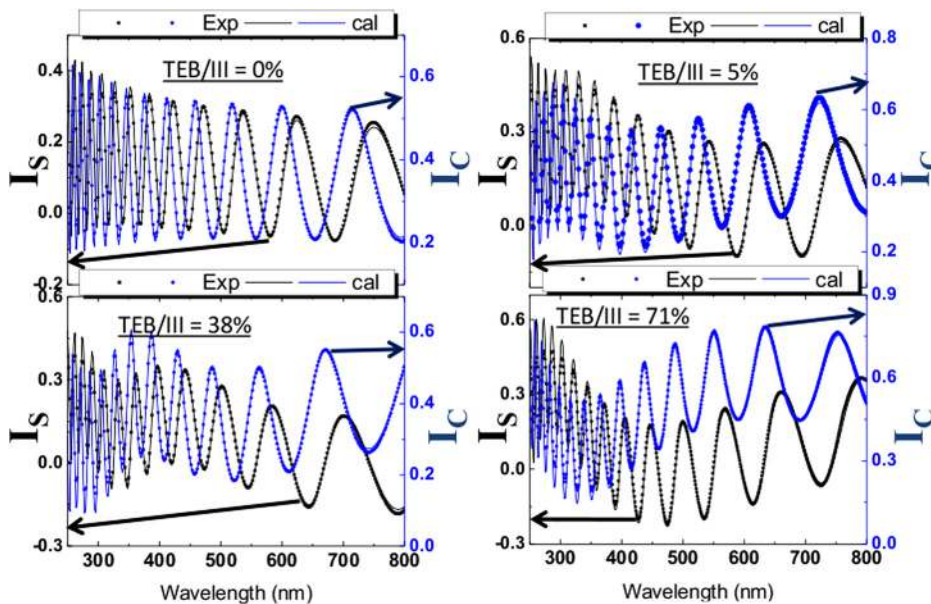


FIG. 2. (Color online) Comparison between measured (dotted lines) and calculated (solid lines) ellipsometric spectra ( $I_s$  and  $I_c$ ) for different TEB/III ratios.

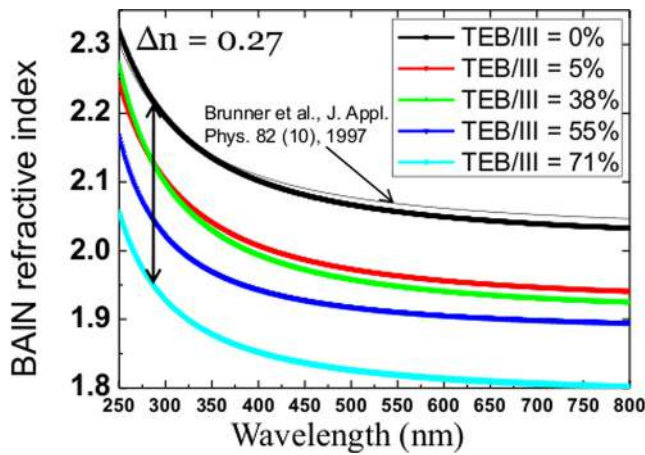


FIG. 3. (Color online) Refractive index of  $B_xAl_{1-x}N$  films for different TEB/III ratio.

confirm the transparency of the BAIN films in the deep UV region. In fact, for 47% boron incorporation, the optical bandgap is only 5.62 eV (220 nm) which theoretically prevent any absorption from occurring in the deep UV DBR structures. The bandgap values could not be confirmed by photoluminescence technique (PL), as the PL peak could not be observed on the BAIN.

As expected, the refractive index contrast between BAIN layer and AlN template increases with the TEB/III ratio, and the AlN refractive index is in excellent agreement with previously reported data.<sup>14</sup> At 300 nm, the BAIN/AlN structure grown for a TEB/III ratio of 71% achieves a refractive index contrast of more than 0.25, which is higher than  $Al_{0.5}Ga_{0.5}N$ /AlN structure based on AlGaIn refractive index data reported by Brunner *et al.*<sup>14</sup>

As a result of the high refractive index contrast (exceeding 0.27 at 280 nm) and the BAIN transparency (Table I), improved DBRs based on BAIN/AlN structures with high reflectivity can be theoretically achieved in the deep UV region. In addition, with the BAIN/AlN structure, our calculation shows that 20 periods are needed to achieve 99% reflectivity and large bandwidth DBR as compared to conventional AlGaIn/AlN DBRs which need more than 30 pairs.

Next, a series of BAIN/AlN DBRs were grown on AlN template substrates. The BAIN/AlN DBRs structures were designed with a target center wavelength located within 250–350 nm. The design was based on BAIN and AlN as the low/high refractive index layer and the BAIN/AlN thicknesses were designed to be quarter-wave layers. In order to compare the reflectivity and bandwidths, the number of stacks in the DBRs was varied from 6 to 24 and the solid phase boron incorporation was also varied. Careful examinations by Nomarski optical microscopy showed that all the BAIN/AlN DBR structures were completely crack-free over the full sample area.

TABLE I. Calculation of the boron content and optical bandgaps as a function of the TEB/III ratio in the different BAIN layers.

TEB/III (%)	0	5	38	55	71
Boron content (%)	0	3.5	26	35	47
Eg (eV)	6.28	6.06	5.80	5.68	5.62

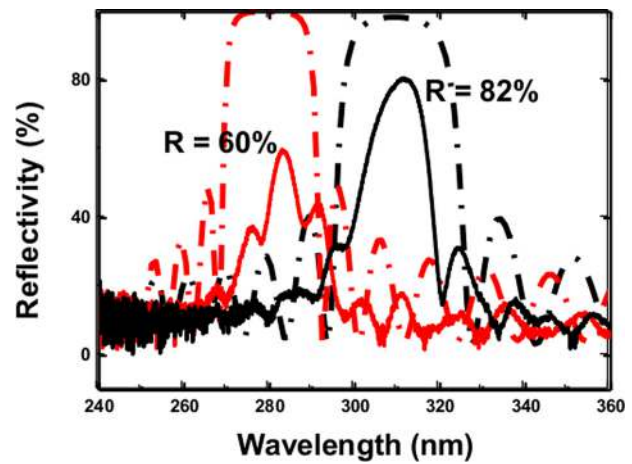


FIG. 4. (Color online) Experimental (dotted lines) and simulated (solid lines) reflectivity spectrum of 18/24-pair BAIN/AlN DBR. The spectra are centered at 311 nm and 282 nm, respectively.

Figure 4 shows the experimental and calculated reflectivity spectra of 18- and 24-period  $B_{0.47}Al_{0.53}N$ /AlN DBR structures. The experimental reflectivities were measured by Fourier Transform Infrared Spectroscopy (FTIR). At 311 nm, a reflectivity of 82% and a bandwidth of 20 nm were obtained for only 18 periods. The 24-pair DBRs reaching a deep UV wavelength of 282 nm exhibit a peak reflectivity of 60% and a bandwidth of 16 nm. In spite of the achieved high reflectivity, the measured reflectivity is lower than the predicted reflectivity (97% and 99%) using the transfer matrix method<sup>15,16</sup> based on the experimental refractive index values obtained in this study. In order to understand the difference between the experimental and simulated reflectivities, DBR samples were examined by transmission electron microscopy (TEM).

Figure 5 shows a Z-contrast TEM image of an 18-period DBR structure. The bottom is the AlN template and the upper is the DBR. One can see that the interface between bright (AlN) and dark (BAIN) layers are quite rough, and we

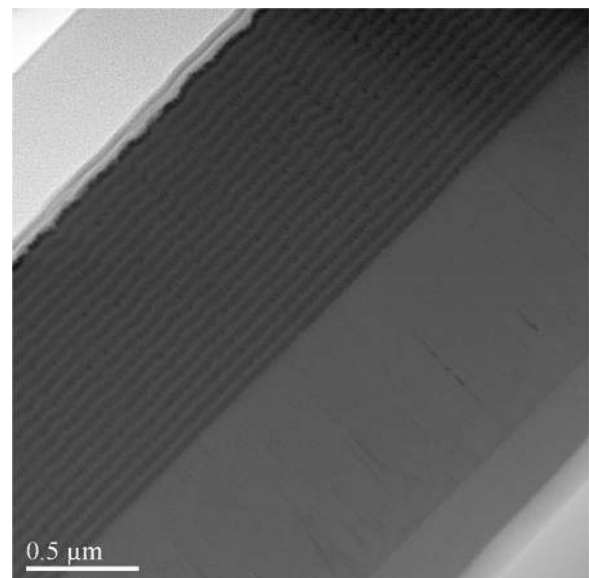


FIG. 5. Cross section of an 18-pair BAIN/AlN stack grown on AlN template.



believe this is the main reason for the discrepancy between the measured and theoretically expected peak reflectivity of our samples. Furthermore, the several nm of surface roughness of the DBR structure observed by AFM leads to optical scattering loss, which is also one of the factors leading to the mismatch between the calculated and measured reflectivity spectra. The thickness of each BAIN/AlN bilayer measured from the TEM micrograph (34 nm/32 nm) coincides with the designed parameters and the targeted values expected from the growth rates of AlN and BAIN. Additionally, EDX analysis in the DBR structures revealed the presence of boron in the AlN layers suggesting a BAIN/BAIN DBR structure instead of the expected BAIN/AlN stack. This feature implies a reduction of the refractive index contrast which consequently decreases the peak reflectivities.

The achieved high peak reflectivity of our BAIN-based DBRs is promising. With an improvement of BAIN material quality through the growth condition optimization, 90% reflectivity in the deep UV region should be achievable. Additionally, following the demonstrated results on BAIN-based DBRs, the growth of strain-compensated BAIN/AlGaIn mirror in the UV range is of particular interest. These structures can take advantage of strain compensation and also the improved refractive index contrast. As a consequence, higher reflectivity with a minimum number of periods and a large bandwidth could be achieved.

In summary, the strong dependence of refractive index on increasing boron content and the BAIN transparency have enabled the development of BAIN/AlN DBRs for applications at deep UV wavelengths. We have reported a

282 nm-centered DBR stack with a reflectivity of 60%. The optimization of BAIN-based DBR structures may enable an innovative approach to deep UV photonics devices such as deep UV VCSELs, back reflectors in light emitting diodes (LEDs) or resonant cavity photodetectors, as well as distributed Bragg confinement layers in edge emitting lasers.

- <sup>1</sup>R. G. Banal, F. Mitsuru, and K. Yoichi, *Appl. Phys. Lett.* **99**, 011902 (2011).
- <sup>2</sup>J. Zhang, H. Zhao, and N. Tansuet, *Appl. Phys. Lett.* **98**, 171111 (2011).
- <sup>3</sup>J. F. Carlin, J. Dorsaz, E. Feltin, R. Butté, N. Gandjean, and M. Illegems, *Appl. Phys. Lett.* **86**, 031107 (2005).
- <sup>4</sup>E. Feltin, J. F. Carlin, J. Dorsaz, G. Christmann, R. Butté, M. Laügt, M. Illegems, and N. Gandjean, *Appl. Phys. Lett.* **88**, 051108 (2006).
- <sup>5</sup>H. Kim-Chauveau, P. de Mierry, J.-M. Chauveau, and J.-Y. Duboz, *J. Cryst. Growth* **316**, 30 (2011).
- <sup>6</sup>J. Zhang, S. Kutlu, G. Liu, and N. Tansu, *J. Appl. Phys.* **110**, 043710 (2011).
- <sup>7</sup>C. Moe, Y. Wu, J. Piprek, J. Speck, S. DenBaars, and D. Emerson, *Phys. Status Solidi A* **203**, 1915 (2006).
- <sup>8</sup>J. Xiao-Li, J. Ruo-Lian, X. Zi-Li, L. Bin, Z. Jian-Jun, L. Liang, H. Ping, Z. Rong, Z. You-Dou, and G. Hai-Mei, *Chin. Phys. Lett.* **24**, 1735 (2007).
- <sup>9</sup>S. Watanabe, T. Takano, K. Jinen, J. Yamamoto, and H. Kawanishi, *Phys. Status Solidi C* **0**, 2691 (2003).
- <sup>10</sup>S. Gautier, C. Sartel, S. Ould-Saad, J. Martin, A. Sirenko, and A. Ougazzaden, *J. Cryst. Growth* **298**, 428 (2007).
- <sup>11</sup>G. E. Jellison, Jr. and F. A. Modine, *Appl. Phys. Lett.* **69**(3), 371 (1996).
- <sup>12</sup>G. E. Jellison, F. A. Modine, P. Doshi, and A. Rohatgi, *Thin Solid Film* **313**, 193 (1998).
- <sup>13</sup>A. S. Keita, A. En Naciri, F. Delachat, M. Carrada, G. Ferblantier, and A. Slaoui, *J. Appl. Phys.* **107**, 093516 (2010).
- <sup>14</sup>D. Brunner, H. Angerer, E. Bustarret, R. Freudenberger, R. Höpler, R. Dimitrov, O. Ambacher, and M. Stutzmann, *J. Appl. Phys.* **82**, 5090 (1997).
- <sup>15</sup>M. Born and E. Wolf, *Principles of Optics* (Pergamon, New York, 1959).
- <sup>16</sup>P. Yeh, *Optical Waves in Layered Media* (Wiley, New York, 1988).